Rice *HYDROPEROXIDE LYASES* with Unique Expression Patterns Generate Distinct Aldehyde Signatures in Arabidopsis[1]

E.W. Chehab, G. Raman, J.W. Walley, J.V. Perea, G. Banu[2], S. Theg, and K. Dehesh*

Section of Plant Biology, University of California, Davis, California 95616

HYDROPEROXIDE LYASE (*HPL*) genes encode enzymes that catalyze the cleavage of fatty acid hydroperoxides into aldehydes and oxoacids. There are three *HPL*s in rice (*Oryza sativa*), designated *OsHPL1* through *OsHPL3*. To explore the possibility of differential functional activities among these genes, we have examined their expression patterns and biochemical properties of their encoded products. Transcript analysis indicates that these genes have distinct patterns and levels of expression. *OsHPL1* is ubiquitously expressed, *OsHPL2* is expressed in the leaves and leaf sheaths, whereas *OsHPL3* is wound inducible and expressed exclusively in leaves. *Os*HPLs also differ in their substrate preference as determined by in vitro enzyme assays using 9-/13-hydroperoxy linolenic and 9-/13-hydroperoxy linoleic acids as substrates. *Os*HPL1 and *Os*HPL2 metabolize 9-/13-hydroperoxides, whereas *Os*HPL3 metabolizes 13-hydroperoxy linolenic acid exclusively. Sequence alignments of the HPL enzymes have identified signature residues potentially responsible for the substrate specificity/preference of these enzymes. All three *Os*HPLs are chloroplast localized as determined by chloroplast import assays and green fluorescent protein (GFP) fusion studies. Aldehyde measurements in transgenic Arabidopsis (*Arabidopsis thaliana*) plants overexpressing individual *Os*HPL-GFP fusions indicate that all rice HPLs are functional in a heterologous system, and each of them generates a distinct signature of the metabolites. Interestingly, these aldehydes were only detectable in leaves, but not in roots, despite similar levels of *Os*HPL-GFP proteins in both tissues. Similarly, there were undetectable levels of aldehydes in rice roots, in spite of the presence of *OsHPL1* transcripts. Together, these data suggest that additional tissue-specific mechanism(s) beyond transcript and HPL enzyme abundance, regulate the levels of HPL-derived metabolites.

Plants have evolved multiple signal transduction pathways to ensure effective responses to biotic and abiotic challenges, as well as to developmental stimuli. One such pathway is the oxylipin pathway, which upon activation by environmental and developmental inputs, induces the de novo synthesis of biologically active compounds called oxylipins (Feussner and Wasternack, 2002; Howe and Schilmiller, 2002). The biosynthesis of these compounds is initiated by the coordinated action of lipases and lipoxygenases, leading to the oxygenation of free polyunsaturated fatty acids (FAs), mainly linoleic and α-linolenic acids, and the generation of 9- or 13-hydroperoxy FAs (9-/13-hydroperoxyoctadecatrienoic acid [9-/13-HPOT] and 9-/13-hydroperoxyoctadecadienoic acid [9-/13-HPOD]). These hydroperoxy FAs are metabolized by a group of cytochrome P450 enzymes present in different branch pathways, to generate the oxylipins (Feussner and Wasternack, 2002). Among the oxylipin branch pathways, the allene oxide synthase (AOS) and the hydroperoxide lyase (HPL) are considered to be the two major critical plant stress response pathways. These two branches compete for the same substrates, and are responsible for the production of lipid-based compounds involved in signaling as well as antimicrobial and antifungal activities. Much of the research to date on plant oxylipins is focused on the jasmonate family of molecules generated by the AOS branch pathway (Howe and Schilmiller, 2002). By contrast, the HPL branch pathway responsible for production of aldehydes and corresponding alcohols is not fully characterized.

The first gene encoding HPL was cloned and characterized from green bell pepper (*Capsicum annuum*; Matsui et al., 1996). Sequence homology and electron paramagnetic resonance spectra classified HPL as a member of the cytochrome P450 family (Matsui et al., 1996; Nelson, 1999; Noordermeer et al., 2001). Within this family, HPLs are grouped into two subfamilies depending on their substrate specificities, 13-HPLs (CYP74B) and 9-/13-HPLs (CYP74C). The 13-HPLs reported to be present in many plants such as Arabidopsis (*Arabidopsis thaliana*) leaves (Bate et al., 1998), watermelon (*Citrullis vulgaris*) seedlings (Vick and Zimmerman, 1976), tea (*Camellia sinensis*) leaves (Shibata et al., 1995), and green bell peppers (Husson and Belin, 2002), cleave 13-HPOT and 13-HPOD to

[1] This work was supported by Biostar and National Science Foundation grants awarded to K.D.

[2] Present address: Pacific Northwest National Laboratories, P.O. Box 999, Richland, WA 99352.

* Corresponding author; e-mail kdehesh@ucdavis.edu; fax 530–752–5410.

The author responsible for distribution of materials integral to the findings presented in this article in accordance with the policy described in the Instructions for Authors (www.plantphysiol.org) is: K. Dehesh (kdehesh@ucdavis.edu).

Article, publication date, and citation information can be found at www.plantphysiol.org/cgi/doi/10.1104/pp.106.078592.

generate cis-3-hexenal and hexanal, respectively. These C_6 aldehydes are involved in plant signaling as well as defense, and are major contributors to the aroma of many fruits, vegetables, and green leaves (Gardner et al., 1991; Hatanaka, 1993). In addition, 9-/13-HPLs such as those present in cucumber (*Cucumis sativus*; Matsui et al., 2000) and melon (*Cucumis melo*; Tijet et al., 2001), metabolize both 13- and 9-hydroperoxides to produce the C_6 aldehydes and the bactericidal compounds (*E*,*Z*)-2,6-nonadienal and (*E*)-2-nonenal (Cho et al., 2004).

The expression of *HPL* genes and the production of their metabolites in plants are induced by biotic and abiotic stimuli (Bate et al., 1998; Laudert and Weiler, 1998; Matsui et al., 1999; Howe et al., 2000; Ziegler et al., 2001). These metabolites, specifically the C_6 volatiles, have antimicrobial (Croft et al., 1993), antifungal (Hamilton-Kemp et al., 1992), and anti-insect properties (Vancanneyt et al., 2001), suggesting that they play a protective role in plant defense. In fact, the (*E*)-2-hexenal produced in response to bacterial pathogenesis (Croft et al., 1993; Zhao et al., 2005) is described as a volatile antibiotic (Lyr and Banasiak, 1983). Furthermore, these C_6 volatiles are shown to elicit the accumulation of phytoalexin (Zeringue, 1991), inhibit seed germination (Gardner et al., 1990), and act as signals to induce defense-response genes both within as well as between plants (Bate and Rothstein, 1998; Koch et al., 1999; Arimura et al., 2001; De Moraes et al., 2001; Farag and Paré, 2002; Engelberth et al., 2004; Kishimoto et al., 2005).

Many plant species have more than one gene encoding HPL enzymes. For example, *Medicago truncatula* is reported to have two HPLs, whereas alfalfa (*Medicago sativa*) has three (Noordermeer et al., 2000). This variation in the number of genes among plant species may reflect the differential regulation of this pathway and ultimately, the diversity of their responses to various stimuli.

The *HPL* genes appear to be regulated by organ-specific and wound-induced transcriptional activation (Bate et al., 1998; Matsui et al., 1999), as well as by substrate availability (Croft et al., 1993; Matsui et al., 2001; Vancanneyt et al., 2001).

Localization studies of HPL protein by tissue print immunoblot analysis of bell pepper showed that HPL is mainly located in the outer parenchymal cells of the pericarp (Shibata et al., 1995). This is consistent with the HPL-proposed primary role in defense against external invasions. Tissue-specific HPL activity varies between plant species and is developmentally regulated (Vick and Zimmerman, 1976; Gardner et al., 1991; Riley et al., 1996). In cucumber seedlings, the highest HPL activity has been reported in the roots (Hatanaka et al., 1988), whereas in watermelon seedlings and potato (*Solanum tuberosum*), this activity was present in the hypocotyl-root junction and the leaves, respectively (Vick and Zimmerman, 1976; Vancanneyt et al., 2001).

Subcellular localization studies determined that HPLs are membrane proteins with diverse localization patterns. Of the many plant species examined, HPLs have been localized to the microsomes (Matsui et al., 1991; Riley et al., 1996; Pérez et al., 1999), lipid bodies (Mita et al., 2005), outer envelope of chloroplasts (Froehlich et al., 2001), and in some cases, no specific localization in a particular organelle is observed (Phillips and Galliard, 1978; Shibata et al., 1995; Noordermeer et al., 2000).

To examine the differential regulation and potential functional differences between *HPL* gene family members within the same species, we focused on rice (*Oryza sativa*), the model monocot, and cloned three *HPL* genes from this plant. The existence of two of these genes (*OsHPL1* and 2) was recently reported (Kuroda et al., 2005). These authors, however, restricted their investigation to the in vitro activity assays of the encoded products and classified both enzymes as 9-/13-HPLs. Here we report the cloning of an additional HPL gene (*OsHPL3*), and further establish that the three *OsHPL* genes have distinct patterns and levels of expression. In addition, we determine that the encoded proteins of all three *OsHPL*s are functional in a heterologous system, with each enzyme generating a distinct profile of aldehydes. We also show that despite the presence of *HPL* transcripts and their encoded products within the roots, the HPL-derived metabolites are below the levels of detection in this tissue. This suggests that additional tissue-specific mechanism(s), beyond transcript and HPL enzyme abundance, regulate the levels of HPL-derived metabolites.

RESULTS

*OsHPL*s Belong to Two Distinct Phylogenetic Clusters

Database searches enabled us to identify three *HPL* genes in rice: *OsHPL1* (AK105964), *OsHPL2* (AK107161), and *OsHPL3* (AY340220), none of which contains any introns. All three genes were isolated and cloned by PCR-based amplification from rice genomic DNA, and their identity was confirmed by sequence analysis. *OsHPL1* (1,533 bp) is predicted to encode a polypeptide of 511 amino acids with a calculated molecular mass of 55 kD. *OsHPL2* (1,503 bp) is predicted to encode a polypeptide of 501 amino acids with a calculated molecular mass of 54 kD. *OsHPL3* (1,464 bp) is predicted to encode a polypeptide of 488 amino acids with a calculated molecular mass of 54 kD. Analysis of the *Os*HPL's deduced amino acid sequences predicted the presence of domain structures typical of cytochrome P450 enzymes, including I- and K-helices, and a heme-binding domain (Heme-BD; Fig. 1A). Further sequence analyses show that *Os*HPL1 and *Os*HPL2 have 84% amino acid identity with each other, and 34% to 45% identity with all other HPLs reported so far. Interestingly however, these HPLs show 42% to 56% amino acid identity with all reported AOSs. On the other hand, *Os*HPL3 shares 34% to 40% and 34% to 72% amino acid identity with AOSs and HPLs, respectively. *Os*HPL3 shares 43% amino acid identity with *Os*HPL1 and *Os*HPL2.

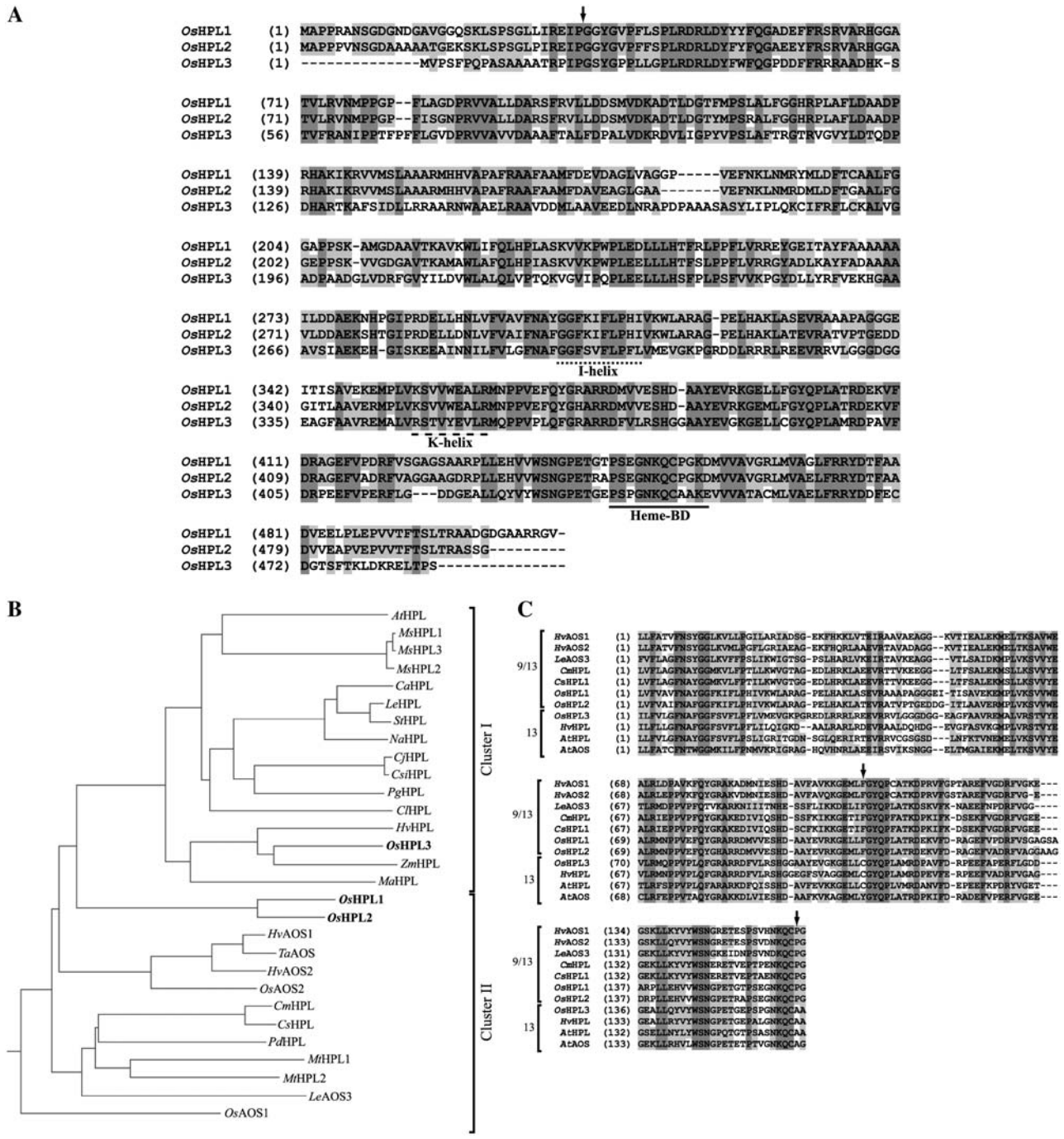

Figure 1. Sequence alignment and phylogenetic analysis. A, Alignment of the deduced amino acid sequences of the *Os*HPLs. The dotted and dashed lines denote the I- and K-helices, respectively. The solid line denotes the Heme-BD. The arrow indicates the position of the conserved Arg residue. B, Phylogenetic tree of all reported HPLs and selected AOSs based on their full-length deduced amino acid sequences. C, Alignment of the deduced amino acid sequences for the catalytic domain of a selected number of characterized AOSs and HPLs. The putative signature amino acid residues are denoted by arrows. Plant species and accession numbers are: *At*HPL, Arabidopsis (AAC69871); *Ms*HPL1, alfalfa (CAB54847); *Ms*HPL3, alfalfa (CAB54849); *Ms*HPL2, alfalfa (CAB54848); *Ca*HPL, green bell pepper (AAK27266); *Le*HPL, tomato (AAF67142); *St*HPL, potato (CAC44040); *Na*HPL, *Nicotiana attenuata* (CAC9156); *Cj*HPL, *Citrus jambhiri* (BAC55161); *Csi*HPL, tea (AAO72740); *Pg*HPL, *Psidium guajava* (AAK15070); *Cl*HPL, *Citrullus lanatus* (AA412570); *Hv*HPL, *Hordeum vulgare* (CAC82980); *Os*HPL3, rice (AY340220); *Zm*HPL, *Zea mays* (AAS47027); *Ma*HPL, *Musa acuminata* (CAB86384); *Os*HPL1, rice (AK105964); *Os*HPL2, rice (AK107161); *Hv*AOS1, *H. vulgare* (CAB86384); *Ta*AOS, *Triticum aestivum* (AAO43440); *Hv*AOS2, *H. vulgare* (CAB86383); *Os*AOS2, rice (AAL17675); *Cm*HPL, melon (AAM66137); *Cs*HPL, cucumber (AAF64041); *Pd*HPL, almond (CAE18065); *Mt*HPL1, *M. truncatula* (CAC86898); *Mt*HPL2, *M. truncatula* (CAC86899); *Le*AOS3, tomato (AAN76867); *Os*AOS1, rice (BAD08330); *At*AOS, Arabidopsis (CAA63266).

Because of the higher percentage of amino acid sequence identity between *Os*HPL1 and 2, and the AOSs, phylogenetic analyses were performed on both branch pathway enzymes, using the Vector NTI 9.0 Align X program. For simplicity however, here we present the phylogenetic analyses performed on a selected number of characterized AOSs. Based on these findings, the HPL enzymes are divided into two clusters. Members within each cluster not only share sequence similarity, but also a common substrate preference (Fig. 1B). *Os*HPL3 belongs to cluster I where all the characterized members are classified as 13-HPLs (CYP74B; Bate et al., 1998; Howe et al., 2000). *Os*HPL1 and *Os*HPL2 belong to cluster II whose characterized members metabolize 9-/13-hydroperoxides (CYP74C; Matsui et al., 2000; Itoh et al., 2002).

The AOS enzymes within the CYP74A subfamily are also classified, based on their substrate preference, into 13- and 9-/13-AOSs (Laudert et al., 1996; Schneider and Schreier, 1998; Howe et al., 2000; Maucher et al., 2000; Sivasankar et al., 2000; Feussner and Wasternack, 2002; Maucher et al., 2004). To explore the possible presence of a common distinctive signature residue(s) involved in the substrate specificity and/or preference of HPLs and AOSs, we further performed multiple sequence alignments of the catalytic sites of all characterized members of these enzymes. These results show that *Os*HPL1 and *Os*HPL2 together with all the characterized 9-/13-AOSs and 9-/13-HPLs contain a Pro within the Heme-BD sequence, PS(E/P)G(N/D)K(Q/I)C(A/P)(G/A)K(D/N) (Fig. 1C). Whereas, *Os*HPL3 similar to all the other characterized 13-AOSs and 13-HPLs, exhibits a Pro to Ala transition. In addition, within the stretch of amino acid sequences between the K-helix and Heme-BD, (L/I)(F/C)G(Y/F)(Q/R)(P/K), there is an invariable Cys residue present in 13-hydroperoxide-preferring enzymes, which is replaced by a Phe in *Os*HPL1, *Os*HPL2, as well as other reported 9-/13-AOSs and 9-/13-HPLs (Fig. 1C). These invariable amino acids potentially constitute a catalytic or a structural component responsible for the substrate preference of the enzymes within their respective phylogenetic cluster.

Unique Expression Patterns of *OsHPL*s

The expression levels and patterns of *OsHPL*s in roots, leaf sheaths, and leaves of mechanically wounded and unwounded rice plants were analyzed by semiquantitative reverse transcription (RT)-PCR using gene-specific oligonucleotides (Fig. 2, A and B). These data show that *OsHPL1* is expressed in all tissues examined, *OsHPL2* transcripts are present in the leaves and leaf sheaths but are absent in the roots, and the *OsHPL3* transcripts are detected exclusively in the leaves (Fig. 2B). Furthermore, there is no significant wound induction in the transcript levels of *OsHPL1* and *OsHPL2*, whereas wounding caused a notable increase in *OsHPL3* transcript levels. Abundance of the control transcript, *Actin*, remains constitutive in all tissues. Reactions without the RT step failed to amplify the *OsHPL*s. These data clearly indicate that the amplified products are not the result of contamination caused by the genomic DNA.

The same analyses were also performed on partially submerged rice plants, simulating natural growing conditions. These data were identical to those from nonsubmerged plants (Fig. 2B; data not shown).

Aldehydes Are Exclusively Present in the Leaves of Rice

The HPL-derived metabolites were analyzed by gas chromatography/mass spectrometry (GC/MS) in different rice tissues obtained from the same batches of plant material previously used in the transcriptional profiling experiments. These data show that the main constituents of the HPL pathway metabolites are the C_6 aldehydes (hexanal and hexenal), and that C_9 aldehydes (nonenal and nonadienal) are below the levels

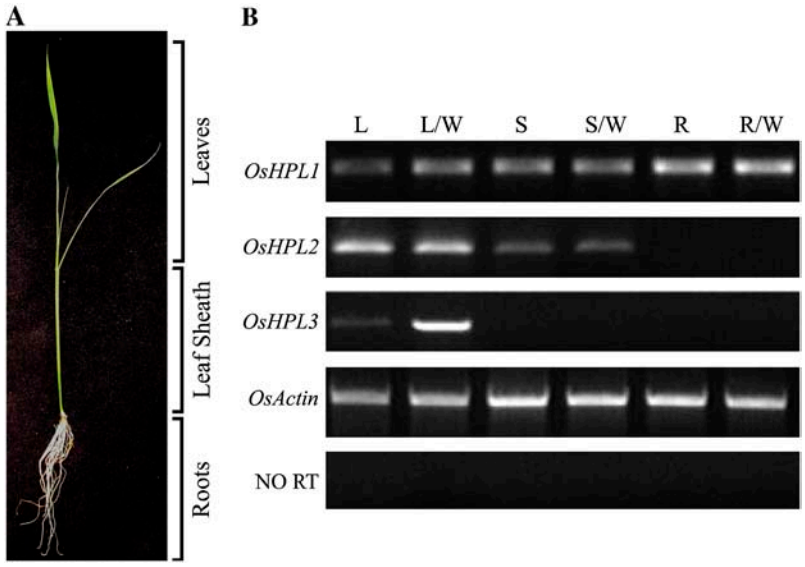

Figure 2. Transcriptional profiling of *OsHPL* genes. A, Four-week-old rice seedling indicating the various tissues used in the assays. B, Steady-state transcript levels of *OsHPL1*, *OsHPL2*, and *OsHPL3* in unwounded and wounded leaves (L and L/W), leaf sheaths (S and S/W), and roots (R and R/W). Rice actin (*OsActin*) was used as the control. Control reactions without the RT step are also shown.

of detection (Fig. 3, A and B). Among these two C_6 aldehydes, hexenal is the predominant metabolite with its level, under all the experimental conditions examined, being approximately 5-fold higher than the hexanal level. Furthermore, these data clearly indicate that stress induced by wounding leads to a 5- and 10-fold increase in the levels of hexenal and hexanal in either nonsubmerged or partially submerged plants, respectively, as compared to the corresponding basal levels in the leaves. Interestingly, no aldehydes are detected in the leaf sheaths or in the roots, despite the presence of *OsHPL* transcripts in these tissues (Figs. 2B and 3, A and B). Moreover, a lack of notable induction in the *OsHPL1* and 2 transcripts, in response to stress, does not correlate with the increase in the levels of C_6 aldehydes in the leaves. On the other hand, the stress-inducible increase in the abundance of *OsHPL3* transcripts correlates well with the increase in the levels of these aldehydes. This suggests that stress-inducible induction of the levels of aldehydes in rice leaves is primarily due to the activity of the *OsHPL3*-encoded product (Fig. 3, A and B).

*Os*HPLs Are Chloroplast Localized

Sequence analyses of *Os*HPLs using ChloroP 1.1 (http://www.cbs.dtu.dk) predicted the localization of *Os*HPL1, 2, and 3 to the chloroplasts. To experimentally validate these predictions, we examined the ability of the in vitro translated *Os*HPLs to bind to isolated pea (*Pisum sativum*) chloroplasts in the presence of ATP. In contrast to *OsHPL3*, the in vitro translated products of *OsHPL1* and *OsHPL2* failed to bind to the organelle (Fig. 4A). Fractionation of the chloroplast import reaction showed that *Os*HPL3 is absent from the soluble stromal fraction, but is associated with the envelopes. The presence of a lighter band detected in the thylakoids membrane fraction is most likely due to the contamination by the bulk envelopes within which the *Os*HPL3 resides (Fig. 4A). Furthermore, the appearance of a lower M_r form of *Os*HPL3 upon import indicates the proteolytic removal of an N-terminal transit peptide.

To further examine the in vivo localizations of *Os*HPLs, a C-terminal green fluorescent protein (GFP) translational fusion construct for each *Os*HPL, expressed under the control of the cauliflower mosaic virus 35S promoter, was introduced into Arabidopsis plants. The transgenic plants containing the *Os*HPL-GFP fusion constructs were used to isolate protoplasts that were subsequently imaged with an epifluorescent microscope. As shown (Fig. 4B), the fluorescence signals of all *Os*HPLs-GFP fusions were found in chloroplasts, as identified by imaging the autofluorescence of their chlorophyll. Control panels show that GFP protein expressed from a construct lacking the HPL fusion does not localize to the same organelle. These results confirmed that all three *Os*HPLs are localized to the chloroplasts.

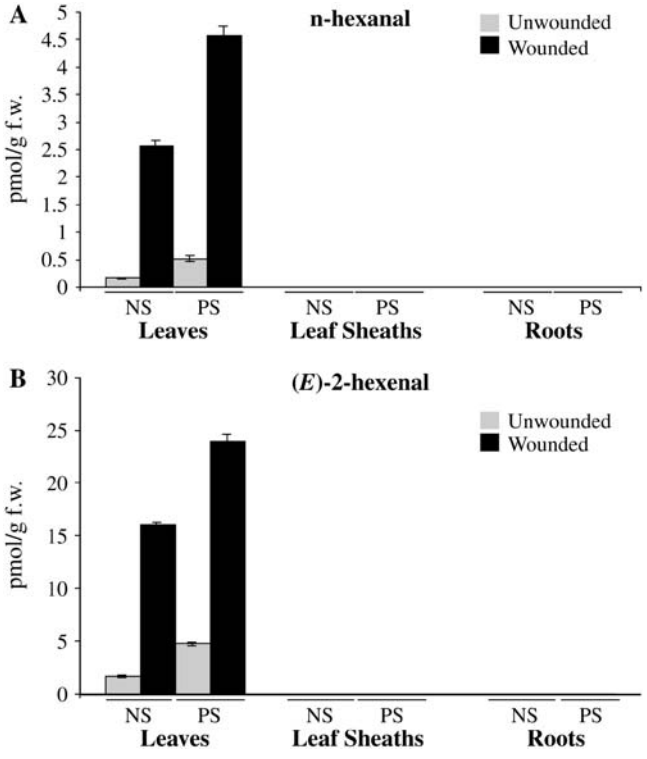

Figure 3. Profiling of HPL-derived metabolites in rice. The levels of *n*-hexanal (A) and (*E*)-2-hexenal (B) in wounded and unwounded leaves, leaf sheaths, and roots of rice plants grown under nonsubmerged (NS) or partially submerged (PS) conditions. Histograms are the average of triplicate assays and the bars indicate SD.

Substrate Preference of Recombinant *Os*HPLs Matches Their Phylogenetic Cluster

To examine substrate preference of the recombinant *Os*HPLs in an in vitro enzyme assay, we had to identify the cleavage site of the signature peptides of these chloroplast-localized enzymes. Since the chloroplast import assays of *Os*HPL1 and 2 were not successful, we could not confirm the presence or absence of a cleavable transit peptide for these enzymes. Based on previous reports, most outer envelope-localized proteins lack a cleavable signature sequence (Cline and Henry, 1996). For example, it has been shown that *Le*HPL, localized to the outer envelope of the chloroplasts, lacks a detectable cleavable transit peptide (Froehlich et al., 2001). We therefore postulated that *Os*HPL1 and 2, similar to *Le*HPL, may lack a cleavable transit peptide. Hence, we cloned the full-length open reading frames of *Os*HPL1 and *Os*HPL2 into an expression vector. In the case of *Os*HPL3, we cloned both the full-length *Os*HPL3 (*Os*HPL3-FL) as well as its predicted mature portion lacking a 15-amino acid N-terminal variable sequence (*Os*HPL3) into an expression vector. Determination of the N-terminal amino acid of the *Os*HPL3 mature enzyme was based on two observations; first, the prediction of size difference of the in vitro translated product before and after

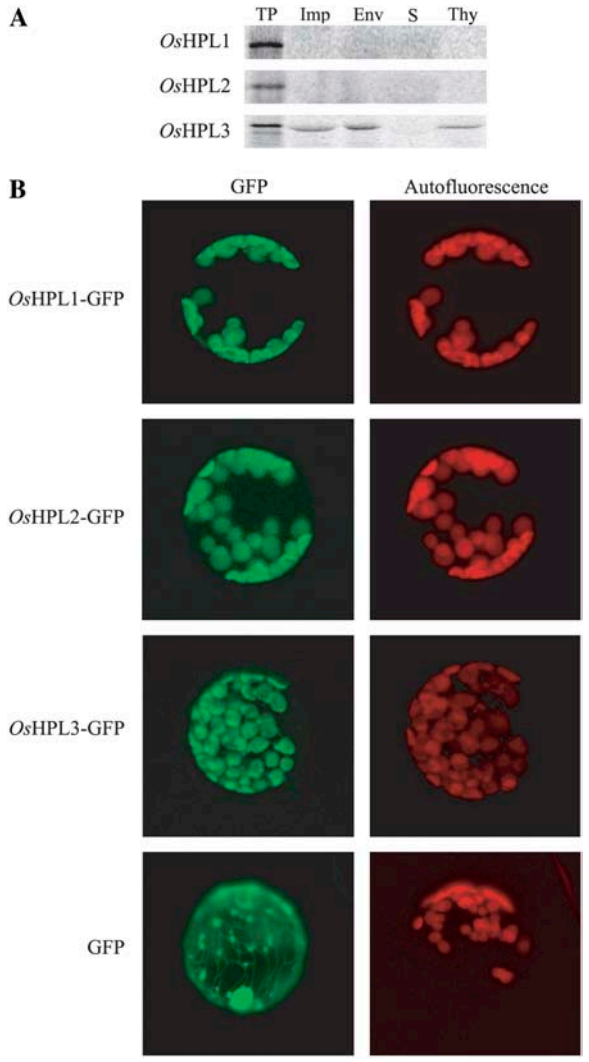

Figure 4. Localization of *Os*HPLs to the chloroplasts. A, The in vitro transcribed and translated [^{35}S]-labeled *Os*HPLs before (TP) and after (Imp) import into pea chloroplasts. In contrast to *Os*HPL3, both *Os*HPL1 and 2 failed to bind. Fractionation of *Os*HPL3 import assays into envelope (Env), stroma (S), and thylakoids (Thy) fractions show the localization of the labeled polypeptide to the envelopes. The lighter band detected in the thylakoids is potentially due to the contamination with chloroplast envelopes. B, Single protoplasts isolated from transgenic lines overexpressing *Os*HPL1-GFP, *Os*HPL2-GFP, *Os*HPL3-GFP, and GFP show that all fusion proteins are chloroplast localized. Autofluorescence of the chlorophyll is depicted in red.

import to the chloroplast, as shown (Fig. 4A). Second, based on the sequence alignment studies, we identified the conserved residue Arg-16 as the start of the mature polypeptide (Fig. 1A). All the *Os*HPL recombinant proteins contain a 6xHis tag sequence at their N termini.

To examine the substrate preferences of each of the recombinant *Os*HPLs, we performed the enzyme assays with crude lysates harboring the recombinant proteins in the presence of either 9-/13-HPOT or 9-/13-HPOD as substrates.

These data in agreement with those previously published (Kuroda et al., 2005), clearly show that *Os*HPL1 and *Os*HPL2 metabolize 13-HPOT/D and 9-HPOT/D equally well with no apparent substrate preference. In contrast, *Os*HPL3 is exclusively active on 13-HPOT (Fig. 5, A–D). Furthermore, both *Os*HPL3-FL and *Os*HPL3 show similar substrate preference profiles, suggesting that the presence of the transit peptide does not interfere with the recognition of the substrate (Fig. 5, C and D). The control *Escherichia coli* lysate from cells expressing insertless expression vectors did not contain any detectable hydroperoxy FA metabolizing activity (Fig. 5E).

Recombinant *Os*HPLs Catalyze Cleavage of 13-HPOT into (*E*)-2-Hexenal

To identify the catalytic properties of *Os*HPL enzymes, previously identified as *Os*AOSs (Agrawal et al., 2004; Haga and Iino, 2004), we performed HPL-specific assays using the recombinant enzymes produced in *E.coli*. The *E. coli* extracts from cells expressing *Os*HPLs were incubated with 13-HPOT, and the resulting products were examined by GC/MS analysis (Fig. 6). These data clearly show that these enzymes catalyze the cleavage of 13-HPOT into (*E*)-2-hexenal (mass-to-charge ratios = 98, 83, 69, and 55). No such product was detected in assays performed with the *E. coli* lysate harboring the insert-free vector control. These data clearly establish that these rice genes indeed encode functional HPL enzymes. In addition, these data together with the in vitro substrate preference assays and in conjunction with the phylogenetic analyses establish the identity *Os*HPL1 and *Os*HPL2 as members of CYP74C, and *Os*HPL3 as a member of CYP74B subfamilies.

*Os*HPLs Are Functional in a Heterologous System

The in vivo functionality of the *Os*HPLs in a heterologous system was examined by generation of transgenic Arabidopsis plants overexpressing *Os*HPLs-GFP fusion proteins. The expression levels of *Os*HPL-GFP fusion in each line was determined by western-blot analysis using commercially available GFP monoclonal antibodies. Lines with similar levels of *Os*HPLs-GFP together with the wild type and transgenic Arabidopsis expressing GFP alone were employed in GC/MS analyses to determine the composition and the levels of the HPL-derived metabolites in leaves (Fig. 7, A and B). These analyses indicated that the levels and profiles of the C_6 aldehydes in wild-type leaves are similar to those from the GFP overexpressers (data not shown). For simplicity, we have only included the data obtained from the latter line. Transgenic Arabidopsis overexpressing the *Os*HPLs-GFP fusions accumulates considerably higher levels of C_6 aldehydes, namely hexenal and hexanal in the leaves, as compared to those from the GFP-overexpressing lines (Fig. 7B). Specifically, the plants expressing *Os*HPL1-, *Os*HPL2-,

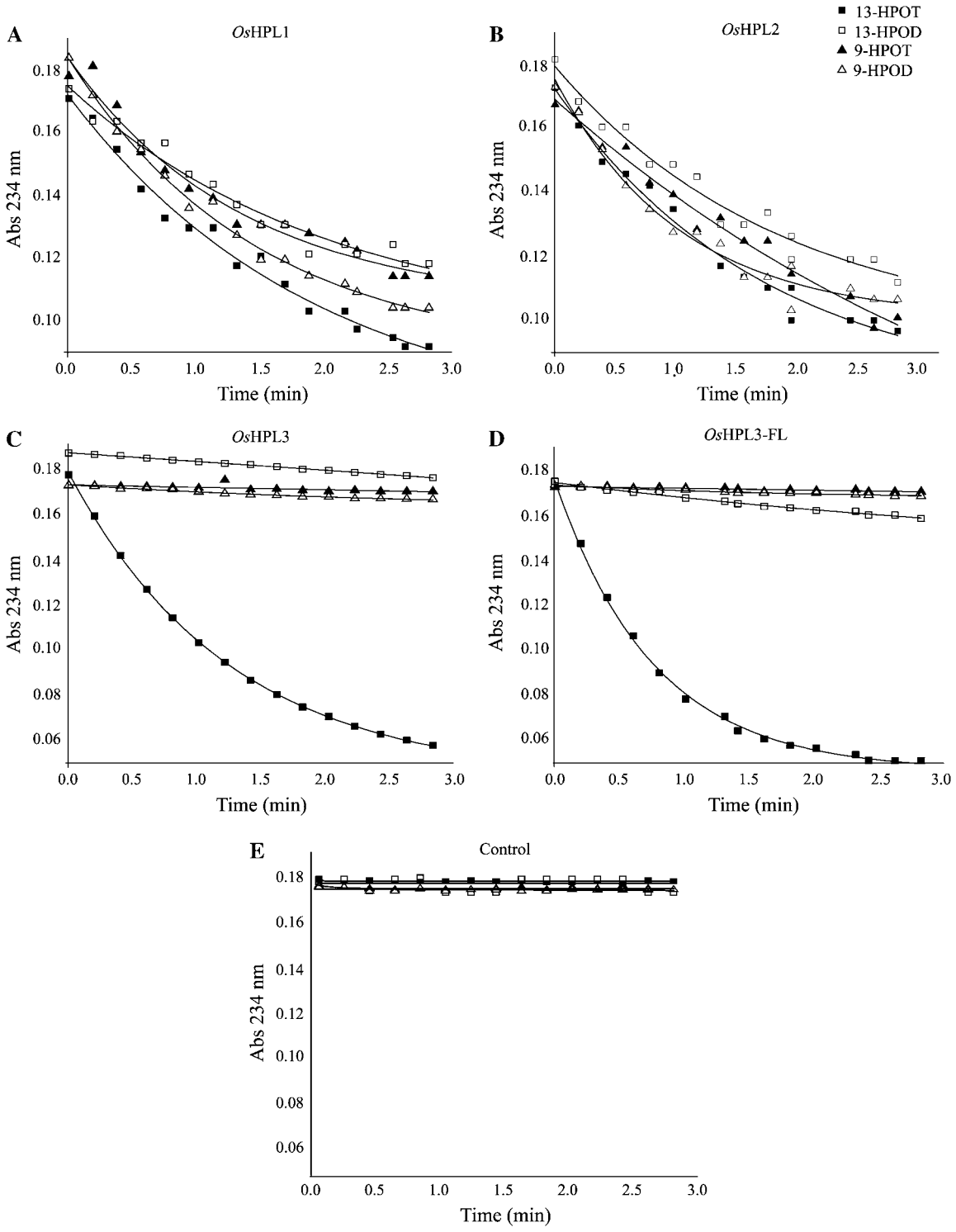

Figure 5. In vitro enzyme activity assays of recombinant *Os*HPLs using 9-/13-hydroperoxides. Utilization of 9-/13-hydroperoxides by recombinant *Os*HPL1 (A), *Os*HPL2 (B), *Os*HPL3 (C), *Os*HPL3-FL (D), and control (E) *E. coli* lysate were measured by monitoring the loss of absorbance of substrate at 234 nm. Each assay was based on at least three independent studies each performed with three replicates.

and *Os*HPL3-GFP fusions generate 25-, 82-, and 4-fold more hexanal, and 18-, 60-, and 68-fold more hexenal, respectively, as compared to GFP expressing Arabidopsis. In all instances, the predominant C_6 aldehyde is hexenal. The highest fold difference between hexenal and hexanal (168-fold) is observed in *Os*HPL3-GFP lines. Plants overexpressing *Os*HPL1- and *Os*HPL2-GFP fusions contain 7- and 8-fold more hexenal than hexanal, respectively. The profile of the *Os*HPL3-GFP-derived metabolites in the corresponding transgenic

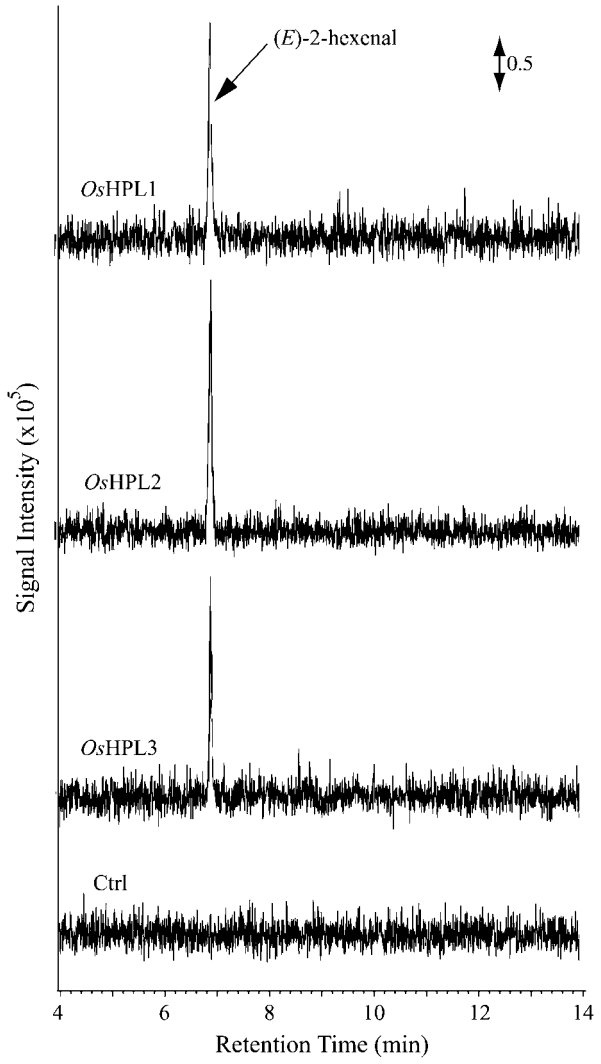

Figure 6. HPL-specific assays performed with the recombinant enzymes. *E. coli* extracts expressing *Os*HPL1, *Os*HPL2, or *Os*HPL3 catalyze the cleavage of 13-HPOT into (*E*)-2-hexenal, whereas the vector control (Ctrl) does not cleave 13-HPOT as reflected by the absence of detectable levels of (*E*)-2-hexenal. Double-headed arrow represents a scale for signal intensity.

plants reflects the observed in vitro substrate specificity of the *Os*HPL3 recombinant enzyme (Figs. 5, C and D and 7B). Interestingly however, C_9 aldehydes were not detected in Arabidopsis plants overexpressing either *Os*HPL1 or *Os*HPL2, even though both enzymes metabolized 9- and 13-hydroperoxides with equal efficacy in vitro. Furthermore, in spite of the presence of comparable levels of the *Os*HPL-GFP fusion proteins in the leaves, these lines differ in their total levels of aldehydes (Figs. 7, A and B). Plants overexpressing *Os*HPL2-GFP and *Os*HPL3-GFP have comparable levels of total aldehydes, and they both contain 3-fold higher levels than the *Os*HPL1-GFP line.

Leaves from the nontransgenic control were devoid of any immunoreactive bands (Fig. 7A).

Aldehydes Are Absent in Transgenic Arabidopsis Roots

The metabolic profiling of HPL-derived metabolites in different rice tissues clearly indicated that the aldehydes are below the levels of detection in roots, in spite of the presence of *OsHPL1* transcripts in this tissue. Due to the lack of availability of an HPL antibody that could recognize HPLs in general and *Os*HPL1 in particular, we could not correlate the presence of the transcript to the translated product. The availability of the transgenic Arabidopsis line producing *Os*HPL1-GFP fusion, however, provided us with the enabling tool to examine the presence of aldehydes in the roots in correlation to the enzyme levels. The selection of *Os*HPL1-GFP transgenic plants for these studies was based on the expression pattern analysis, which established the presence of the *OsHPL1* transcripts in rice roots (Fig. 2B). The expression of *Os*HPL1 in the transgenic roots was confirmed by image analysis using an epifluorescent microscope (Fig. 8A). The levels of *Os*HPL1 expressed in roots versus that present in the

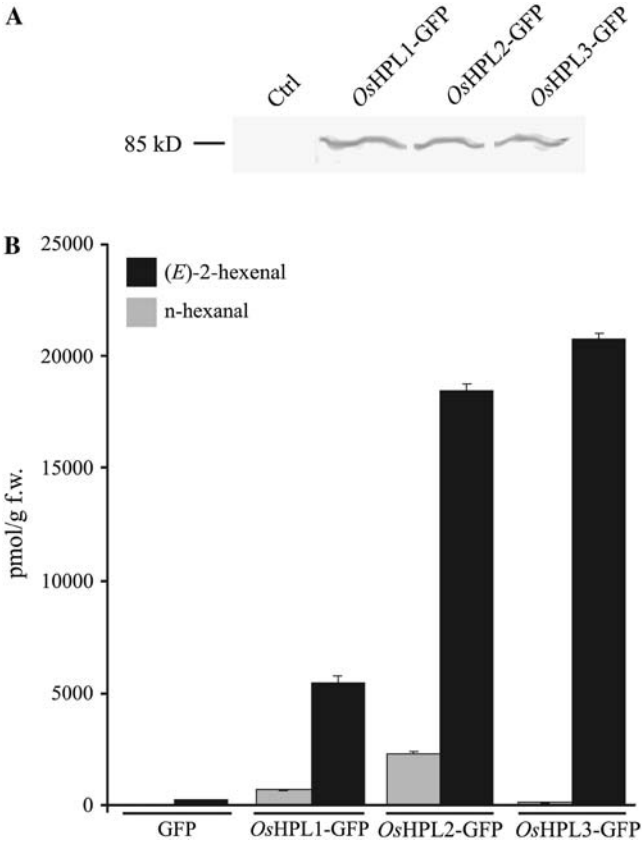

Figure 7. In vivo functionality of *Os*HPLs in Arabidopsis. A, Western-blot analysis performed on equal amount of proteins (20 μg) obtained from nontransgenic control (Ctrl), and transgenic Arabidopsis leaves overexpressing *Os*HPL-GFP fusions (*Os*HPL1 through 3-GFP). Blots were probed with anti-GFP monoclonal antibodies. There are no immunoreactive bands in the control section. B, The levels of (*E*)-2-hexenal and *n*-hexanal in the leaves of the transgenic Arabidopsis plants expressing similar levels of the fusion polypeptides. Histograms are the average of triplicate assays and the bars indicate SD.

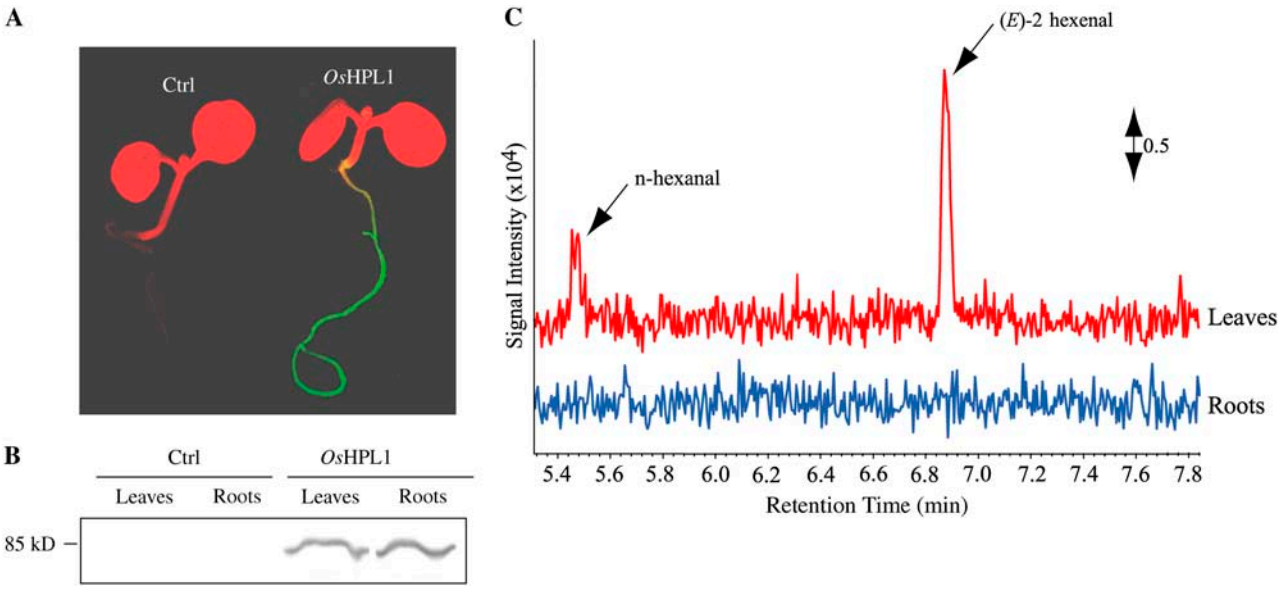

Figure 8. Comparison of aldehyde levels in roots and leaves of transgenic Arabidopsis. A, Side-by-side comparison of nontransgenic control (Ctrl) and *Os*HPL1-GFP-overexpressing Arabidopsis seedlings shows exclusive presence of the green fluorescence in the roots of the transgenic plant. The green fluorescence in the transgenic leaves is masked by the chlorophyll autofluorescence. B, Western-blot analysis performed on equal amount of proteins (20 μg) from the roots and leaves obtained from the same transgenic as well nontransgenic control plants (Ctrl). Blots were probed with anti-GFP monoclonal antibodies. There are no immunoreactive bands in the control section. C, GC/MS chromatograms showing the levels of *n*-hexanal and (*E*)-2-hexenal in leaf (red) and root (blue) tissue from transgenic Arabidopsis overexpressing *Os*HPL1-GFP. Double-headed arrow represents a scale for signal intensity.

leaves of the same transgenic plant were determined by western-blot analysis using the GFP monoclonal antibodies. Those data show that *Os*HPL1 protein is expressed at similar levels in the root and leaves of the transgenic plant (Fig. 8B). Interestingly however, similar to the rice tissue, the aldehydes were below the levels of detection in roots of the transgenic Arabidopsis. In contrast, the leaves collected from the same plant, contain considerable levels of hexenal and hexanal as indicated on the GC/MS chromatograph (Fig. 8C).

Roots and leaves from the nontransgenic control were devoid of any immunoreactive bands (Fig. 8B).

DISCUSSION

We have cloned three *HPL* genes, *OsHPL1* through *OsHPL3*, from the model monocot rice. These genes are differentially regulated as determined by their respective spatial expression patterns as well as the basal- and wound-inducible steady-state transcript levels. The *OsHPL1* transcript is present in leaves, roots, and leaf sheaths, whereas that of *OsHPL2* is not detectable in the roots. *Os*HPL3 transcript is present exclusively in the leaves. Moreover, wound-inducible induction of the mRNA abundance is most notable for *OsHPL3*. These data prompted us to compare promoter sequences of the *OsHPLs* for the presence of regulatory elements that may unravel the molecular basis of the differential spatial expression patterns and response to wounding. The *OsHPL1* promoter contains two identical, unique cis-elements (ACTTTA) present at 49 and 222 bp upstream of the transcriptional start site. This motif is reported to be critical for the expression of *rolB* oncogene in leaves, stems, and roots of tobacco (*Nicotiana tabacum*; Baumann et al., 1999). Thus, the presence of this motif may explain the molecular basis for the ubiquitous presence of *OsHPL1* transcripts in all tissues examined. The unique cis-element in *OsHPL2* is the (CAANNNNATC) motif present 400 bp upstream of the transcriptional start site. This regulatory element is conserved among the clock-regulated, light-harvesting complex protein genes that are not expressed in roots or Bright-Yellow 2 nongreen culture cells (Piechulla et al., 1998). Therefore, it is tempting to speculate that, similar to the *OsAOS1* gene (Haga and Iino, 2004), *OsHPL2* is regulated by light and thus is absent in nonphotosynthetic organs. The *OsHPL3* promoter contains a unique cis-element (AACGTGT) present 95 bp upstream of its transcriptional start site. This element is known as *Ext*A cis-element present in the promoter region of a wound-inducible *extensin* gene in *Brassica napus* (Elliott and Shirsat, 1998). The cis-element shared by all *OsHPL*s is the W box (TTGAC), a motif necessary for the binding of WRKY DNA-binding proteins responsible for the activation of pathogen-induced genes (Yu et al., 2001).

Detailed amino acid sequence comparison in conjunction with the examination of the substrate specificity/preference of the enzymes led to the grouping of

*Os*HPLs into two phylogenetic clusters. *Os*HPL1 and *Os*HPL2, though highly similar to each other, are more similar to AOSs than to all the other HPLs. In fact, due to these higher levels of amino acid sequence identity with AOSs, *Os*HPL1 and 2 were previously clustered within the AOS family of enzymes and were designated as *Os*AOS3 and 4 (Agrawal et al., 2004; Haga and Iino, 2004). However, HPL-specific assays with the recombinant *Os*HPL1 and 2 enabled us to confirm their identities as HPL enzymes (Fig. 6).

Based on the detailed sequence analysis, *Os*HPL1 and 2 form their own clade nested between HPLs and AOSs. Subsequent enzyme activity assays showed that *Os*HPL1 and 2, similar to closely related enzymes in the AOS and HPL group cluster, metabolize 9-/13-HPOT/D and thus belong to the CYP74C subfamily enzymes. We therefore placed *Os*HPL1 and 2 into cluster II, where the enzymes, in addition to their respective amino acid identity, also share similar activity profiles on 9-/13-hydroperoxides. *Os*HPL3 has higher percent amino acid identity with other HPLs than with AOSs. This enzyme belongs to cluster I, where in addition to sequence identity, the enzymes exclusively metabolize 13-hydroperoxides. Thus, in contrast to *Os*HPL1 and 2, *Os*HPL3 belongs to CYP74B subfamily enzymes. In fact, *Os*HPL3 is the only enzyme known to be active exclusively on 13-HPOT, as all the other characterized 13-HPLs metabolize both 13-HPOT and 13-HPOD (Bate et al., 1998; Howe et al., 2000). Although the physiological relevance of this exclusivity is currently unclear, one may postulate that the substrate specificity of *Os*HPL3 enhances plant stress response by diverting adequate levels of 13-HPOT substrate from the competing AOS branch into the HPL branch pathway.

Detailed examination of multiple alignments of the catalytic regions of these enzymes led to the identification of two potential signature residues within the consensus sequences that may play a critical structural or functional role in determining the substrate preference of the enzymes. One potential signature is within the (L/I)(F/C)G(Y/F)(Q/R)(P/K) consensus sequence, where the C residue in 13-hydroperoxide-preferring enzymes is replaced by the more bulky and hydrophobic F residue present in all 9-/13-hydroperoxide-preferring enzymes. The second potential signature is within the Heme-BD [(PS(E/P)G(N/D)K(Q/I)C(A/P)(G/A)K(D/N)], where the nonreactive A residue present in all the characterized 13-hydroperoxide-preferring enzymes is replaced by the P in the 9-/13-hydroperoxides enzymes. The potential function of these signature residues in determining the substrate profile of these cytochrome P450 enzymes is yet to be examined.

The *Os*HPLs are similar in their subcellular localizations. A combination of import assays and GFP-fusion studies confirmed that *Os*HPL3 is similar to *Le*HPL, a member of CYP74B subfamily that is localized to the chloroplasts (Froehlich et al., 2001). Among the 9-/13-HPLs, *Pd*HPL from almonds (*Prunus dulcis*) is reported to be targeted to the endomembrane system and the lipid bodies (Mita et al., 2005). The other 9-/13-HPLs such as *Cm*HPL and *Cs*HPL, have not yet been localized. *Os*HPL1 and 2 are localized to chloroplasts as demonstrated by GFP-fusion studies. Interestingly however, the *Os*HPL1 and 2 chloroplast import assays were unsuccessful. This failure might be due to the absence of chemical components required for the import of these polypeptides, or absence of other factors such as posttranslational modifications of the transit peptide. This hypothesis is supported by a previous finding demonstrating the importance of phosphorylation of the transit peptide in chloroplast import (May and Soll, 2000).

In parallel with the transcriptional profiling, we also examined the levels of HPL-derived metabolites in rice. These data clearly show the lack of detectable levels of aldehydes in rice leaf sheaths and roots, in spite of the presence of *Os*HPL1 transcripts at levels similar to those in leaves, and the presence of *Os*HPL2 mRNA in the leaf sheaths (Figs. 2B and 3). This suggests additional tissue-specific mechanism(s) regulating the levels of these metabolites at posttranscriptional levels and/or substrate availability. Furthermore, unlike *OsHPL1* and *OsHPL2*, the enhancement of *OsHPL3* transcript levels in response to wounding correlates well with the induction of these aldehydes in leaves, thus suggesting that the *OsHPL3*-encoded enzyme is primarily responsible for the production of HPL-derived metabolites in response to stress (Figs. 2B and 3).

The expression of *Os*HPLs-GFP fusion constructs in Arabidopsis further provided us with the necessary tools to examine the differential functionality of these enzymes in vivo by measuring the profile and levels of aldehydes produced in plants that express similar levels of *Os*HPL enzymes as determined by western-blot analysis using anti-GFP monoclonal antibodies (Fig. 7A). The profiles of the HPL-derived metabolites in the *Os*HPLs-GFP-overexpressing lines are distinct from each other. Specifically, plants overexpressing *Os*HPL3-GFP accumulate significantly higher levels of hexenal and lower levels of hexanal as compared to those overexpressing *Os*HPL1- and *Os*HPL2-GFP (Fig. 7B). Plants with *Os*HPL1- and *Os*HPL2-GFP transgenes generated high levels of hexenal as well as hexanal, which reflect their ability to metabolize both 13-HPOT and 13-HPOD substrates. Although the recombinant *Os*HPL1 and *Os*HPL2 enzymes metabolize 13-hydroperoxides equally well, their expression in the transgenic line resulted in the production of higher levels of hexenal, the products of 13-HPOT, than hexanal, the products of 13-HPOD. This suggests that the availability of substrate regulated by upstream components of the HPL pathway determines the in vivo profiles of the aldehydes. Similarly, the absence of detectable levels of nonenal and nonadienal, derived from 9-hydroperoxides, in these plants also reflects the unavailability of the 9-HPOT/D substrates. In accordance with these data, it is reported that overexpression of *Cs*9HPL in tomato (*Lycopersicon esculentum*) did

not result in detectable levels of nonenal or nonadienal (Matsui et al., 2001). These authors further indicated that the preferential conversion of the free FAs to the 13-hydroperoxides led to a lack of availability of 9-hydroperoxides. Plants overexpressing *Os*HPL3-GFP accumulate significantly higher levels of hexenal than those of the GFP lines. The presence of hexenal as the main HPL-derived metabolite in these *Os*HPL3-GFP lines matched the exclusive in vitro activity of the recombinant *Os*HPL3 on 13-HPOT. The negligible levels of hexanal in the *Os*HPL3-GFP are, however, potentially due to the activity of the endogenous *At*HPL enzyme.

The composition and the levels of the HPL-derived metabolites were examined in plants expressing similar levels of enzymes (Fig. 7, A and B). In spite of similar protein levels, Arabidopsis plants overexpressing *Os*HPL1-GFP contained only one third of the aldehyde levels as compared to each of those overexpressing *Os*HPL2- and *Os*HPL3-GFP. This suggests that in a heterologous system, *Os*HPLs have different activities, with *Os*HPL1 being the least active enzyme.

As stated above, we have established that rice roots do not contain aldehydes in spite of the presence of *OsHPL1* transcripts at levels similar to those in the leaves. To begin to dissect the tissue-specific mechanism(s) involved, we exploited the transgenic Arabidopsis lines, overexpressing *Os*HPL1-GFP under the control of 35S promoter. Our analysis showed that although the roots have similar levels of fusion proteins as compared to the leaves, aldehydes are below the levels of detection in this tissue (Fig. 8, B and C). This is in contrast to previous reports showing the presence of aldehydes in the root tissues of red clover (*Trifolium pratense*) and melon (Kamm and Buttery, 1984; Matsuda et al., 2000). The discrepancy suggests that plants have evolved differently in their ability to generate aldehydes in various tissues. The absence of aldehydes in Arabidopsis and rice is either due to enzyme inhibition, or availability of substrate. Alternatively, these metabolites may be released to the surrounding environment soon after their synthesis in the roots. A precedent for emission of volatiles into the root rhizosphere is reported for the monoterpene 1,8-cineole (Chen et al., 2004; Steeghs et al., 2004). The Arabidopsis plants overexpressing the *Os*HPL-GFP fusions will provide us with the enabling tools to further dissect the tissue-specific mechanism(s) that regulate the levels of HPL-derived metabolites.

MATERIALS AND METHODS

Plant Growth and Wound Treatments

Arabidopsis (*Arabidopsis thaliana*) plants were grown in a 16-h-light/8-h-dark cycle at 22°C. Rice (*Oryza sativa*) L. cv Nipponbare plants were grown at 30°C in a greenhouse, under either nonsubmerged or partially submerged conditions. Rice seeds were germinated in soil and grown for 3 weeks before the seedlings were either submerged in water up to the first leaf, or they were kept in dry conditions. Tissues were collected from 4-week-old rice and Arabidopsis plants for the assays described in this report. Mechanical wounding of leaves and leaf sheaths was performed by puncturing the tissue many times using an 18-gauge needle. Tissues were harvested after 2 h of wounding, immediately frozen in liquid nitrogen, and stored at −80°C until use.

Cloning and Sequence Analysis of Rice HPLs

Since none of the *OsHPL* genes contains introns, genomic DNA isolated from rice L. cv Nipponbare was used for PCR-based amplification of these genes using the following gene-specific oligonucleotides: *OsHPL1* (Forward: 5′-ATAGATATCGCATGCATGGCGCCGCCGCGAGCCAACTCCG-3′ and Reverse: 5′-ATATACGTACTGCAGCGCGCGCCGCCGCTTGACACTATTA-3′), *OsHPL2* (Forward: 5′-ATAGATATCGCATGCATGGCGCCACCGCCAGTGAACTCCG-3′ and Reverse: 5′ATATACGTACTGCAGGCACGTGACGTCGACGTGCGTGCTA-3′), and *OsHPL3* (Forward: 5′-ATAGATATCGCATGCATGGTGCCGTCGTTCCCGCAGCCGG-3′ and Reverse: 5′-ATATACGTACTGCAGGAGAGAATGGCGGCAGCAAAGCTTA-3′). For each amplification, 30 PCR cycles were carried out using a Gene Amp PCR system 9700 (Applied Biosystems) in a 25 μL reaction mix containing 10 mM Tris-HCl (pH 8.3), 50 mM KCl, 1.5 mM $MgCl_2$, 4% dimethyl sulfoxide (DMSO), 100 μM of each dNTP, 500 nM of each forward and reverse primer, 0.625 units of *Taq* DNA polymerase (Invitrogen), and 50 ng of the genomic DNA. Amplification was conducted at 94°C for 1 min, 94°C for 30 s, 55°C for *OsHPL1*, 63°C for *OsHPL2*, and 55°C for *OsHPL3* for 1 min, 72°C for 90 s, and a 10-min extension step at 72°C. The amplified products were resolved by electrophoresis on a 1% (w/v) agarose gel. The band corresponding to each full-length gene was cut, purified using QIAquick Gel extraction kit (Qiagen), and cloned in pCR 2.1-TOPO Vector (Invitrogen) according to the manufacturer's instructions. The identities of these clones were confirmed by DNA sequencing. All DNA as well as polypeptide sequence analyses were performed using Vector NTI advance program 9 (Invitrogen).

Chloroplast Protein Import and Fractionation

Plasmids containing full-length DNA sequence of the *OsHPL*s were linearized by restriction endonuclease digestion at sites 3′ of the coding regions. Transcriptions from the linearized plasmids were performed using either T7 or SP6 (Promega) RNA polymerase. Precursor proteins were synthesized using [^{35}S]Met (Perkin Elmer) in a rabbit reticulocyte lysate (Cline et al., 1985). Intact chloroplasts were isolated from 11- to 12-d-old Little Marvel pea (*Pisum sativum*) seedlings (Musser and Theg, 2000). Import of radiolabeled translation product was carried out in import buffer containing 3 mM ATP and intact chloroplasts corresponding to 20 μg of chlorophyll in a final volume of 60 μL. Chlorophyll concentration was determined as described previously (Arnon, 1949). Reactions were incubated for 20 min at room temperature in the light and were terminated by the addition of 600 μL import buffer. Chloroplasts were pelleted and resuspended in 40 μL sample buffer (62.5 mM Tris pH 6.8, 2% [w/v] SDS, 10% [v/v] glycerol, 0.25% [w/v] bromphenol blue, and 5% [v/v] 2-mercaptoethanol).

For fractionation, chloroplasts were utilized in import assays described above, but in a 300 μL reaction and incubated in light for 40 min. After import, reactions were treated with 200 μL of 0.5 M Na_2CO_3 on ice and in the dark for 15 min. Chloroplasts were then reisolated in 1 mL of 30% Percoll (GE Healthcare Bio-Sciences) by centrifuging at 1,900*g*, and then washed with 1 mL of import buffer. Reactions were resuspended in 80 μL of Tris-EDTA + Suc (10 mM Tricine, pH 7.5, 2 mM EDTA, and 0.6 M Suc). A 20 μL sample was taken as the whole chloroplast fraction (import). The remaining 60 μL were incubated on ice, freeze thawed in a −20°C freezer, and then centrifuged at 200*g* for 5 min. The pellet was resuspended in 40 μL 400 mM Suc, 40 mM Na-MES pH 6.5, 10 mM NaCl, and 5 mM $MgCl_2$ from which 20 μL were taken as the thylakoid fraction. The supernatant was spun in an ultracentrifuge at 100,000*g* for 30 min, and the pellet was resuspended in 40 μL of sample buffer as the envelope fraction. The resulting supernatant was TCA precipitated and resuspended in 40 μL of sample buffer plus 0.5 M Tris, pH 8.0, as the stroma fraction.

All samples were run on 15% acrylamide tris-Gly gels, fixed by a 15 min glacial acetic acid wash, and dried on filter paper. Gels were exposed on phosphor screens and visualized on a Storm Scanner (GE Healthcare Bio-Sciences).

Cloning and Expression of *Os*HPLs

The vector PQE-30 (Qiagen) was used for cloning *OsHPL1* and *2*, while *OsHPL3-FL* and *OsHPL3* were cloned in pDEST17. All constructs contain

His_6-tag fusions at their N termini. For the in-frame fusion of the full-length *OsHPL1* and *OsHPL2* into the expression vector, their respective original constructs generated in pCR 2.1-TOPO vector were digested with *Sph*I and *Pst*I and the resulting fragments were individually subcloned into the *Sph*I/*Pst*I sites of the PQE-30 vector. These plasmids were sequenced and their authenticity was confirmed, after which they were transformed into M15 (pREP4) strain *Escherichia coli*.

OsHPL3-FL and *OsHPL3* were amplified by PCR with oligonucleotides designed for Gateway cloning. Primers used for amplification of *OsHPL3-FL* were: Forward: 5′-CACCATGGTGCCGTCGTTCC-3′ and Reverse: 5′-GCTGGGAGTGAGCTCC-3′. *OsHPL3* was amplified using the following primers: Forward: 5′-CACCCGGCCAATACCGGGG-3′ and Reverse: 5′-GCTGGGAGTGAGCTCC-3′. PCR amplification was conducted as described above with T_m = 52°C, used for *OsHPL3-FL* and *OsHPL3*.

Amplified products were cloned into the pENTR/D-TOPO vector, and subcloned into the Gateway destination vector pDEST17 by a LR reaction (Invitrogen). These plasmids were sequenced and transformed into BL21 *E. coli* cells.

Bacteria transformed with each of the above described plasmids or with the vector alone as the control were grown to an OD_{600} of 0.7 and then induced with 0.5 mM isopropyl β-D-thiogalactopyranoside for 3 h. Cells were sedimented by centrifugation (14,000*g*, 10 min), resuspended in a buffer containing 50 mM sodium phosphate (pH 7.0) and mini protease inhibitor mix (Roche Molecular Biochemicals), and sonicated three times on ice for 15 s and 9 W. Debris was pelleted by centrifugation (17,000*g*, 20 min) and the supernatant was used for the enzyme assays.

GFP Fusion Constructs and Arabidopsis Transformation

GFP fusions for stable expression were constructed by cloning the PCR-amplified, TOPO-cloned, and *Eco*RI-/*Bam*HI-digested fragments of the full length of all three genes into the *Eco*RI/*Bam*HI site of pEZS-NLGFP. Primers were designed to eliminate stop codons and fuse the coding sequences to the 5′ end of the *GFP* gene. For *OsHPL1*, the primers used were: Forward: 5′-ATAGAATTCATGGCGCCGCCGCGAG-3′ and Reverse: 5′-ATAGGATCCGCTACTCCGCGCCGCGCG-3′. For *OsHPL2*, the primers used were: Forward: ATAGAATTCATGGCGCCACCGCCAGT-3′ and Reverse: 5′-ATAGGATCCGCTCCCGACGACGCCCGT-3′. *OsHPL3* was amplified using the following primers: Forward: 5′-ATAGAATTCATGGTGCCGTCGTTCCC-3′ and Reverse: 5′-ATAGGATCCGCGCTGGGAGTGAGCTCCC-3′. PCR amplifications were conducted as described above with a T_m = 55°C used for all genes amplified. GFP fusions for Arabidopsis transformation were created by subcloning the *OsHPL1*, *OsHPL2*, and *OsHPL3* open reading frames from pEZS-NLGFP into the binary vector pMLBart, kindly provided by John Bowman (University of California, Davis) using *Not*I restriction sites with the GFP gene at the C terminus of each gene. The constructs were verified by sequencing, introduced into Agrobacterium EHA101 strain, and used to transform Arabidopsis plants by using the floral-dip method (Clough and Bent, 1998). The T1 plants were germinated on soil. Selection of transgenics was by treating 10- to 12-d-old seedlings with 1:1,000 Finale (the commercial product that is 5.78% glufosinate ammonium) twice a week.

Protoplast Isolation and Fluorescent Microscopy

Protoplast isolation was performed as previously described (Sheen, 2002). Briefly, 10 Arabidopsis leaves expressing the GFP fusions of *Os*HPLs were finely chopped and floated on 10 mL of enzyme solution (10 mM $CaCl_2$, 20 mM KCl, 0.4 M mannitol, and 20 mM MES [pH 5.7]) containing 1.5% (w/v) cellulase R10 (Yakult Honsha), 0.4% macerozyme R10 (Yakult Honsha), and 0.1% bovine serum albumin. The tissue was digested at room temperature in the dark. The digest was filtered using 50 μm nylon mesh and centrifuged at 100*g* for 2 min. The pellet was resuspended in 5 mL of ice-cold washing/incubation buffer (500 mM mannitol, 20 mM KCl, and 4 mM MES [pH 5.7]).

Protoplasts were visualized with a Nikon Eclipse 400 epifluorescence microscope (Nikon). GFP was visualized with a 450 to 490 nm excitation filter, a 495 nm dichroic mirror, and a 500 to 550 nm emission filter. Chlorophyll autofluorescence was visualized with a 528 to 553 nm excitation filter, a 565 nm dichroic mirror, and a 600 to 660 nm emission filter.

Enzyme Assays

The hydroperoxide-metabolizing activity of the recombinant HPLs was measured spectrophotometrically by monitoring the decrease in A_{234} resulting from the disruption of the conjugated diene bond of the substrate (Zimmerman and Vick, 1970). Enzyme assays were performed at room temperature in 1 mL of 50 mM sodium phosphate (pH 7.0) with 20 μL of bacterial extract expressing either *Os*HPL1 or *Os*HPL2, or 1 μL of bacterial extract expressing either *Os*HPL3-FL or *Os*HPL3. Reactions were initiated by the addition of 1 μg of an ethanolic solution of the desired hydroperoxide substrate (9-/13-HPOT and 9-/13-HPOD; Cayman Chemical) to the reaction mixture. These experiments were performed in three replicates for each of the independent enzyme activity assays.

RNA Isolation and Semiquantitative RT-PCR Assays

Total RNA was isolated from leaves, leaf sheaths, and roots of wounded and unwounded rice plants grown in nonsubmerged or partially submerged conditions. RNA extraction was carried out by mixing 150 mg of ground and frozen tissue in 1 mL of TRIzol reagent (Life Technologies). Upon addition of chloroform (250 μL) the extract was vortexed briefly and incubated at room temperature for approximately 15 min. The RNA was subsequently precipitated in the presence of 200 mM NaCl, 133 mM Na-citrate, and 17% (v/v) isopropanol, and pelleted by centrifugation (14,000*g*, 30 min) at 4°C. RNA pellets were washed with ice-cold 70% (v/v) ethanol, air dried, and resuspended in diethyl pyrocarbonate-treated water. Transcriptional profiling of HPLs was based on the semiquantitative RT-PCR assays, conducted using 100 ng of DNaseI-treated RNA.

A 516-bp amplicon was obtained using the following *OsHPL1*-specific primers: Forward: 5′-GGCGAGATCACCATCTCC-3′ and Reverse: 5′-TTATACTCCGCGCCGCG-3′.

A 666-bp amplicon was obtained using the following *OsHPL2*-specific primers: Forward: 5′-ATAGAATTCATGGCGCCACCGCCAGT-3′ and Reverse: 5′-CGCGAGCCACGCCATG-3′.

A 976-bp amplicon was obtained using the following *OsHPL3*-specific primers: Forward: 5′-CCTCAACAGGGCCCCTG-3′ and Reverse: 5′-TTAGCTGGGAGTGAGCTCC-3′.

A 1,134-bp amplicon was obtained using the following *OsActin*-specific primers: Forward: 5′-ATGGCTGACGCCGAGGATATC-3′ and Reverse: 5′-TTAGAAGCATTTCCTGTGCACAAT-3′.

RT-PCR reactions were conducted in a 20 μL reaction mixture containing 50 mM Tris-HCl (pH 8.3), 75 mM KCl, 3 mM $MgCl_2$, 100 mM dithiothreitol, 500 μM of each dNTP, 1 μM of each reverse and forward primer, 200 units of Superscript III RT (Invitrogen), 40 units of RNase Out (Invitrogen), 5% DMSO, and 50 ng RNA for the amplification of the desired cDNA. The RT reactions were carried out at 50°C for 45 min followed by heating the sample to 70°C for 15 min to denature the reverse transcriptase. To amplify the DNA fragments, 2.5 μL of the RT reaction was used in a 25 μL reaction mix containing 10 mM Tris-HCl (pH 8.3), 50 mM KCl, 1.5 mM $MgCl_2$, 4% DMSO, 100 mM of each dNTP, 500 nM of each of the forward and reverse primer, and 0.625 units of *Taq* DNA polymerase (Invitrogen). A total of 27 amplification cycles were performed at 95°C for 1 min, 94°C for 15 s, 50°C for 30 s, 72°C for 45 s, and 10 min of extension step at 72°C. The amplified products were resolved by electrophoresis on 1.0% (w/v) agarose and visualized by ethidium bromide staining. These experiments were repeated three times, resulting in an almost identical data set for each independent study.

Western-Blot Analysis

One hundred milligrams of ground and frozen Arabidopsis tissue overexpressing the *Os*HPL-GFP fusions were boiled for 5 min in 200 μL of 2× SDS sample buffer. The mixture was centrifuged (14,000*g*, 5 min) and the protein content was determined by DC protein assay (Bio-Rad) according to the manufacturer's instructions. Equal amounts of proteins (20 μg) were loaded onto 7% SDS-PAGE. The separated proteins were transferred onto a Poly (vinylidene fluoride) PVDF membrane and probed using anti-GFP monoclonal antibodies (CLONTECH). The blots were finally developed using 0.33 mg/mL nitro blue tetrazolium chloride and 0.165 mg/mL 5-bromo-4-chloro-3-indoyl phosphate in 10 mL of Development buffer (100 mM Tris-HCl [pH 9.5], 100 mM NaCl, and 5 mM $MgCl_2$).

Aldehyde Analysis

To measure the aldehyde levels in the plants, the tissue was collected and frozen in liquid nitrogen. The material was ground rapidly and thoroughly with a pestle, and a weighed amount of the sample was introduced into a

4-mL screw-top Supelco vial containing 500 μL of 1% NaCl. The vial was then rapidly capped with the screw top having a polytetrafluoroethylene/silicone septum, and incubated for 30 min in a water bath at 50°C under continuous stirring. A 60-μm polydimethylsiloxane (PDMS)-coated solid phase micro extraction (SPME; Supelco) was used to measure the aldehydes released from the plant tissue. Measurements were done in triplicates. The headspace was sampled for 30 min with the PDMS-SPME and analyzed by GC-MS. GC-MS analysis was performed using a Hewlett and Packard 6890 series gas chromatograph coupled to an Agilent Technologies 5973 network mass selective detector. An HP-5MS column (30 m $\times$ 0.25 mm, 0.25 μm film thickness) was used with He (37 kPa) as carrier gas. The GC oven temperature was programmed as follows: 5 min 40°C, ramp to 225°C at 15°C/min and no hold time. Mass spectra in the electron impact mode were generated at 70 eV. Injection was performed by thermal desorption of the SPME in the injector at 200°C using the splitless injection mode. The compounds were identified by comparing the GC retention times and mass spectra with those of authentic reference compounds. The headspace was analyzed as described above and peak areas (mass-to-charge ratios 82 and 98) were determined.

The aldehydes were quantified subsequent to careful preparation of calibration curves with *n*-hexanal and (*E*)-2-hexenal as standards. It is important to note that based on our analysis using the PDMS fiber, *n*-hexanal and (*E*)-2-hexenal have similar distribution constants, indicating that the fiber adsorbs these compounds equally well within a 10% marginal error.

Analysis of Products Catalyzed by the Recombinant Enzymes

We performed HPL-specific assays by analysis of the products derived from the recombinant enzymes. These assays were carried out in GC vials at room temperature with *E. coli* lysate (2 mg for *Os*HPL1 and *Os*HPL2, and 1 mg for *Os*HPL3) adjusted to a final volume of 1 mL of 0.1 M Tris-HCl (pH 7.0). Upon addition of 13-HPOT (0.1 mM final concentration) to the sample, the vial was rapidly capped with the screw top having a polytetrafluoroethylene/silicone septum, and incubated for 10 min at 40°C. A 60-μm PDMS microextraction fiber probe was inserted into the headspace of the vial and subsequently the probe was injected into the GC/MS and analysis was performed as described above.

ACKNOWLEDGMENT

We thank Raymond Sheehy for growing and maintaining the rice plants in the New Technologies Research Growers greenhouses.

Received February 2, 2006; revised March 1, 2006; accepted March 2, 2006; published March 10, 2006.

LITERATURE CITED

Agrawal GK, Tamogami S, Han O, Iwahashi H, Rakwal R (2004) Rice octadecanoid pathway. Biochem Biophys Res Commun **317:** 1–15

Arimura G, Ozawa R, Horiuchi J, Nishioka T, Takabayashi J (2001) Plant-plant interactions mediated by volatiles emitted from plants infested by spider mites. Biochem Syst Ecol **29:** 1049–1061

Arnon DI (1949) Copper enzymes in isolated chloroplasts: polyphenoloxidase in *Beta vulgaris.* Plant Physiol **24:** 1–15

Bate NJ, Rothstein SJ (1998) C6-volatiles derived from the lipoxygenase pathway induce a subset of defense-related genes. Plant J **16:** 561–569

Bate NJ, Sivasankar S, Moxon C, Riley JM, Thompson JE, Rothstein SJ (1998) Molecular characterization of an Arabidopsis gene encoding hydroperoxide lyase, a cytochrome P-450 that is wound inducible. Plant Physiol **117:** 1393–1400

Baumann K, De Paolis A, Costantino P, Gualberti G (1999) The DNA binding site of the Dof protein NtBBF1 is essential for tissue-specific and auxin-regulated expression of the rolB oncogene in plants. Plant Cell **11:** 323–334

Chen F, Ro DK, Petri J, Gershenzon J, Bohlmann J, Pichersky E, Tholl D (2004) Characterization of a root-specific Arabidopsis terpene synthase responsible for the formation of the volatile monoterpene 1,8-cineole. Plant Physiol **135:** 1956–1966

Cho MJ, Buescher RW, Johnson M, Janes M (2004) Inactivation of pathogenic bacteria by cucumber volatiles (E,Z)-2,6-nonadienal and (E)-2-nonenal. J Food Prot **67:** 1014–1016

Cline K, Henry R (1996) Import and routing of nucleus-encoded chloroplast proteins. Annu Rev Cell Dev Biol **12:** 1–26

Cline K, Werner-Washburne M, Lubben TH, Keegstra K (1985) Precursors to two nuclear-encoded chloroplast proteins bind to the outer envelope membrane before being imported into chloroplasts. J Biol Chem **260:** 3691–3696

Clough SJ, Bent AF (1998) Floral dip: a simplified method for Agrobacterium-mediated transformation of *Arabidopsis thaliana.* Plant J **16:** 735–743

Croft K, Juttner F, Slusarenko AJ (1993) Volatile products of the lipoxygenase pathway evolved from *Phaseolus vulgaris* (L.) leaves inoculated with *Pseudomonas syringae* pv phaseolicola. Plant Physiol **101:** 13–24

DeMoraes CM, Mescher MC, Tumlinson JH (2001) Caterpillar-induced nocturnal plant volatiles repel nonspecific females. Nature **410:** 577–580

Elliott KA, Shirsat AH (1998) Promoter regions of the extA extensin gene from *Brassica napus* control activation in response to wounding and tensile stress. Plant Mol Biol **37:** 675–687

Engelberth J, Alborn HT, Schmelz EA, Tumlinson JH (2004) Airborne signals prime plants against insect herbivore attack. Proc Natl Acad Sci USA **101:** 1781–1785

Farag MA, Paré PW (2002) C6-green leaf volatiles trigger local and systemic VOC emissions in tomato. Phytochemistry **61:** 545–554

Feussner I, Wasternack C (2002) The lipoxygenase pathway. Annu Rev Plant Biol **53:** 275–297

Froehlich JE, Itoh A, Howe GA (2001) Tomato allene oxide synthase and fatty acid hydroperoxide lyase, two cytochrome P450s involved in oxylipin metabolism, are targeted to different membranes of chloroplast envelope. Plant Physiol **125:** 306–317

Gardner HW, Dornbos DLJ, Desjardins A (1990) Hexanal, trans-2-hexenal, and trans-2-nonenal inhibit soybean, Glycine max, seed germination. J Agric Food Chem **38:** 1316–1320

Gardner HW, Weisleder D, Plattner RD (1991) Hydroperoxide lyase and other hydroperoxide-metabolizing activity in tissues of soybean, Glycine max. Plant Physiol **97:** 1059–1072

Haga K, Iino M (2004) Phytochrome-mediated transcriptional up-regulation of ALLENE OXIDE SYNTHASE in rice seedlings. Plant Cell Physiol **45:** 119–128

Hamilton-Kemp TR, McCracken CTJ, Loughrin JH, Andersen RA, Hildebrand DF (1992) Effect of some natural volatile compounds on the pathogenic fungi *Alternaria alternata* and *Botrytis cinerea.* J Chem Ecol **18:** 1083–1091

Hatanaka A (1993) The biogeneration of green odor by green leaves. Phytochemistry **34:** 1201–1218

Hatanaka A, Kajiwara K, Matsui Z (1988) Concentration of hydroperoxide lyase activity in root of cucumber seedlings. Z Naturforsch **43:** 308–310

Howe GA, Lee GI, Itoh A, Li L, DeRocher AE (2000) Cytochrome P450-dependent metabolism of oxylipins in tomato: cloning and expression of allene oxide synthase and fatty acid hydroperoxide lyase. Plant Physiol **123:** 711–724

Howe GA, Schilmiller AL (2002) Oxylipin metabolism in response to stress. Curr Opin Plant Biol **5:** 230–236

Husson F, Belin JM (2002) Purification of hydroperoxide lyase from green bell pepper (*Capsicum annuum* L.) fruits for the generation of C6-aldehydes in vitro. J Agric Food Chem **50:** 1991–1995

Itoh A, Schilmiller AL, McCaig BC, Howe GA (2002) Identification of a jasmonate-regulated allene oxide synthase that metabolizes 9-hydroperoxides of linoleic and linolenic acids. J Biol Chem **277:** 46051–46058

Kamm JA, Buttery RG (1984) Root volatile components of red clover: identification and bioassay with the clover root borer (Coleoptera: Scolytidae). Environ Entomol **13:** 1427–1430

Kishimoto K, Matsui K, Ozawa R, Takabayashi J (2005) Volatile C6-aldehydes and Allo-ocimene activate defense genes and induce resistance against *Botrytis cinerea* in *Arabidopsis thaliana.* Plant Cell Physiol **46:** 1093–1102

Koch T, Krumm T, Jung V, Engelberth J, Boland W (1999) Differential induction of plant volatile biosynthesis in the lima bean by early and late intermediates of the octadecanoid-signaling pathway. Plant Physiol **121:** 153–162

Kuroda H, Oshima T, Kaneda H, Takashio M (2005) Identification and functional analyses of two cDNAs that encode fatty acid 9-/13-hydroperoxide lyase (CYP74C) in rice. Biosci Biotechnol Biochem **69:** 1545–1554

Laudert D, Pfannschmidt U, Lottspeich F, Hollander-Czytko H, Weiler EW (1996) Cloning, molecular and functional characterization of *Arabidopsis thaliana* allene oxide synthase (CYP 74), the first enzyme of the octadecanoid pathway to jasmonates. Plant Mol Biol **31:** 323–335

Laudert D, Weiler EW (1998) Allene oxide synthase: a major control point in *Arabidopsis thaliana* octadecanoid signalling. Plant J **15:** 675–684

Lyr H, Banasiak L (1983) Alkenals, volatile defense substances in plants, their properties and activities. Acta Phytopathol Acad Sci Hung **18:** 3–12

Matsuda Y, Toyoda H, Sawabe A, Maeda K, Shimizu N, Fujita N, Fujita T, Nonomura T, Ouchi S (2000) A hairy root culture of melon produces aroma compounds. J Agric Food Chem **48:** 1417–1420

Matsui K, Fukutomi S, Wilkinson J, Hiatt B, Knauf V, Kajwara T (2001) Effect of overexpression of fatty acid 9-hydroperoxide lyase in tomatoes (*Lycopersicon esculentum* Mill.). J Agric Food Chem **49:** 5418–5424

Matsui K, Shibutani M, Hase T, Kajiwara T (1996) Bell pepper fruit fatty acid hydroperoxide lyase is a cytochrome P450 (CYP74B). FEBS Lett **394:** 21–24

Matsui K, Toyota H, Kajiwara T, Kakuno T, Hatanaka A (1991) Fatty acid hydroperoxide cleaving enzyme, hydroperoxide lyase, from tea leaves. Phytochemistry **30:** 2109–2113

Matsui K, Ujita C, Fujimoto S, Wilkinson J, Hiatt B, Knauf V, Kajiwara T, Feussner I (2000) Fatty acid 9- and 13-hydroperoxide lyases from cucumber. FEBS Lett **481:** 183–188

Matsui K, Wilkinson J, Hiatt B, Knauf V, Kajiwara T (1999) Molecular cloning and expression of Arabidopsis fatty acid hydroperoxide lyase. Plant Cell Physiol **40:** 477–481

Maucher H, Hause B, Feussner I, Ziegler J, Wasternack C (2000) Allene oxide synthases of barley (*Hordeum vulgare* cv. Salome): tissue specific regulation in seedling development. Plant J **21:** 199–213

Maucher H, Stenzel I, Miersch O, Stein N, Prasad M, Zierold U, Schweizer P, Dorer C, Hause B, Wasternack C (2004) The allene oxide cyclase of barley (*Hordeum vulgare* L.)—cloning and organ-specific expression. Phytochemistry **65:** 801–811

May T, Soll J (2000) 14-3-3 proteins form a guidance complex with chloroplast precursor proteins in plants. Plant Cell **12:** 53–64

Mita G, Quarta A, Fasano P, De Paolis A, Di Sansebastiano GP, Perrotta C, Iannacone R, Belfield E, Hughes R, Tsesmetzis N, et al (2005) Molecular cloning and characterization of an almond 9-hydroperoxide lyase, a new CYP74 targeted to lipid bodies. J Exp Bot **56:** 2321–2333

Musser SM, Theg SM (2000) Proton transfer limits protein translocation rate by the thylakoid DeltapH/Tat machinery. Biochemistry **39:** 8228–8233

Nelson DR (1999) Cytochrome P450 and the individuality of species. Arch Biochem Biophys **369:** 1–10

Noordermeer MA, Van Dijken AJ, Smeekens SC, Veldink GA, Vliegenthart JF (2000) Characterization of three cloned and expressed 13-hydroperoxide lyase isoenzymes from alfalfa with unusual N-terminal sequences and different enzyme kinetics. Eur J Biochem **267:** 2473–2482

Noordermeer MA, Veldink GA, Vliegenthart JF (2001) Spectroscopic studies on the active site of hydroperoxide lyase: the influence of detergents on its conformation. FEBS Lett **489:** 229–232

Pérez AG, Sanz C, Olias R, Olias JM (1999) Lipoxygenase and hydroperoxide lyase activities in ripening strawberry fruits. J Agric Food Chem **47:** 249–253

Phillips DR, Galliard T (1978) Flavor biogenesis: partial purification and properties of a fatty acid hydroperoxide cleaving enzyme from fruits of cucumber. Phytochemistry **17:** 355–358

Piechulla B, Merforth N, Rudolph B (1998) Identification of tomato Lhc promoter regions necessary for circadian expression. Plant Mol Biol **38:** 655–662

Riley JM, Willemot C, Thompson JE (1996) Lipoxygenase and hydroperoxide lyase activities in ripening tomato fruit. Postharvest Biol Technol **7:** 97–107

Schneider C, Schreier P (1998) Catalytic properties of allene oxide synthase from flaxseed (*Linum usitatissimum* L.). Lipids **33:** 191–196

Sheen J (2002) Phosphorelay and transcription control in cytokinin signal transduction. Science **296:** 1650–1652

Shibata Y, Matsui K, Kajiwara T, Hatanaka A (1995) Purification and properties of fatty acid hydroperoxide lyase is a cytochrome P450. Plant Cell Physiol **36:** 147–156

Sivasankar S, Sheldrick B, Rothstein SJ (2000) Expression of allene oxide synthase determines defense gene activation in tomato. Plant Physiol **122:** 1335–1342

Steeghs M, Bais HP, de Gouw J, Goldan P, Kuster W, Northway M, Fall R, Vivanco JM (2004) Proton-transfer-reaction mass spectrometry as a new tool for real time analysis of root-secreted volatile organic compounds in Arabidopsis. Plant Physiol **135:** 47–58

Tijet N, Schneider C, Muller BL, Brash AR (2001) Biogenesis of volatile aldehydes from fatty acid hydroperoxides: molecular cloning of a hydroperoxide lyase (CYP74C) with specificity for both the 9- and 13-hydroperoxides of linoleic and linolenic acids. Arch Biochem Biophys **386:** 281–289

Vancanneyt G, Sanz C, Farmaki T, Paneque M, Ortego F, Castanera P, Sanchez-Serrano JJ (2001) Hydroperoxide lyase depletion in transgenic potato plants leads to an increase in aphid performance. Proc Natl Acad Sci USA **98:** 8139–8144

Vick BA, Zimmerman DC (1976) Lipoxygenase and hydroperoxide lyase in germinating watermelon seedlings. Plant Physiol **57:** 780–788

Yu D, Chen C, Chen Z (2001) Evidence for an important role of WRKY DNA binding proteins in the regulation of NPR1 gene expression. Plant Cell **13:** 1527–1540

Zeringue HJ Jr (1991) Effect of C6 to C9 alkenals on aflatoxin production in corn, cottonseed, and peanuts. Appl Environ Microbiol **57:** 2433–2434

Zhao J, Davis LC, Verpoorte R (2005) Elicitor signal transduction leading to production of plant secondary metabolites. Biotechnol Adv **22:** 283–333

Ziegler J, Keinanen M, Baldwin IT (2001) Herbivore-induced allene oxide synthase transcripts and jasmonic acid in Nicotiana attenuata. Phytochemistry **58:** 729–738

Zimmerman DC, Vick BA (1970) Hydroperoxide isomerase: a new enzyme of lipid metabolism. Plant Physiol **46:** 445–453